Investigating the effect of solvent boiling temperature in P3HT:PCBM diffusive bilayer solar cells

Varun Vohra,[1] Bernhard Dörling,[2] Koichi Higashimine[3] and Hideyuki Murata[4]

[1]*Department of Engineering Science, University of Electro-Communications, Chofu, Tokyo 182-8585, Japan*

[2] *Institut de Ciència de Materials de Barcelona (ICMAB-CSIC), Campus de la UAB, 08193 Bellaterra, Spain*

[3] *Nano-material Technology Center, Japan Advanced Institute of Science and Technology, Nomi, Ishikawa 923-1292, Japan*

[4] *School of Materials Science, Japan Advanced Institute of Science and Technology, Nomi, Ishikawa 923-1292, Japan*

E-mail: varun.vohra@uec.ac.jp

Using chlorobenzene as a base solvent for the deposition of the poly(3-hexylthiophene-2,5-diyl) (P3HT) layer in P3HT: Phenyl-C_{61}-butyric acid methyl ester diffusive bilayer solar cells, we investigate the influence of the resulting active layer morphologies when adding small amounts of higher boiling point solvents of a similar chemical nature. The results demonstrate that the crystallinity of the P3HT films as well as the vertical donor-acceptor gradient in the active layer can be tuned using this approach. The use of higher boiling point solvents improved all photovoltaic parameters and resulted in a 32% increase in power conversion efficiency.

Among the emerging technologies which may replace silicon as the future generation of solar cells, organic donor-acceptor based active layers represent a promising candidate with single cell efficiencies now overcoming the milestone efficiency of 10%.[1-4] Recent advances in the field of polymer solar cells (PSC) have greatly emphasized the importance of the formation of a vertical concentration gradient to enhance the charge transport and collection efficiencies.[1,2,5] Most of the PSC are based on the bulk heterojunction (BHJ-SC) concept (mixture of electron donor and acceptor molecules) as it favors the generation of a large quantity of holes and electrons through intimate mixing of both materials (increase in donor-acceptor interface).[6] However, a fair amount of studies have also focused on a concept referred to as diffusive bilayers (DB-PSC) where the donor and acceptor molecules are sequentially deposited from orthogonal solutions.[5-14] The solvent used for acceptor layer deposition, namely, dichloromethane (DCM), does not entirely dissolve the underlying polymer donor layer but allows for the acceptor fullerene derivative to diffuse through it generating a concentration gradient within the active layer.[13] Previous studies have, however, demonstrated that depending on the crystallinity of the bottom polymer layer, the fullerene derivative can diffuse throughout the whole active layer, therefore leading to active layer morphologies very similar to those of BHJ-SC.[7] DB-SC based on high efficiency polymers exhibit power conversion efficiencies in the range or higher than their BHJ-SC counterparts as long as charge transport towards the wrong electrode is inhibited by the formation of donor and acceptor layers at the interfaces with the anode and the cathode, respectively. [9,11]

The objective of this study is to observe the effect of increasing solvent boiling point on the polymer and active layer morphologies. Simple AFM characterizations of the polymer film surface, together with the UV-Vis absorption spectra, demonstrate the increase in crystallinity of the polymer upon addition of higher boiling point solvents. A meticulous study of the vertical concentration gradient in the various active layers allowed us to correlate

the device performances to the active layer morphologies confirming that an optimal concentration gradient results in an efficient charge transport and collection (increase in Jsc and FF) and therefore enhanced efficiencies. In particular, we observed that the solid solvent, 1,3,5-trichlorobenzene (s-TCB), which acts as a crystallization agent,[15] leads to a PCE increase of 32% when compared to the reference low boiling point solvent PSC.

The devices (and samples) for characterization were prepared as follows:

Pre-patterned indium tin oxide (ITO) covered glass substrates were cleaned by subsequent sonication in acetone, detergent, deionized water, isopropanol and then exposed to isopropanol vapor. After 30 min of exposure in a UV-O_3 surface treatment chamber, a 40 nm thick layer of poly(3,4-ethylenedioxythiophene) poly(styrenesulfonate) (PEDOT:PSS) is deposited by spin-coating a commercial suspension (Clevios AI4083) at a speed of 4000 rpm for 30s. The substrates are then annealed at 200°C for 10 min followed by sequential deposition in a nitrogen-filled glovebox of the poly(3-hexylthiophene-2,5-diyl) (P3HT) solutions in chlorinated benzene derivative solvents and a phenyl-C_{61}-butyric acid methyl ester (PCBM) solution in DCM. In order to evaluate the influence of the increasing boiling point solvents in the P3HT solution without changing the device process parameters, chlorobenzene (CB) was used as base solvent to which the following solvents were added at a concentration of 100mg/ml (P3HT concentration of 30 mg/ml of base CB):

1. CB (reference cells)
2. 1,2-dichlorobenzene (DCB)
3. 1,3,5-trichlorobenzene (s-TCB)
4. 1,2,4-trichlorobenzene (l-TCB)

It is expected that the final film crystallinity will be determined by the additive and not the carrier solvent even for small amounts, since the total drying time is mostly dependent on the highest boiling solvent. The P3HT solutions were spin-coated at a speed of 2500 rpm for 60s

to form thin P3HT films with an average thickness of around 70 nm. The PCBM solution in DCM was then spin-coated on top of the P3HT films at a speed of 4000 rpm for 10s. It is worth mentioning that the 100 mg/ml was chosen as it corresponds to the optimized conditions for s-TCB; however, similar trends can be observed at various additional solvent concentrations.

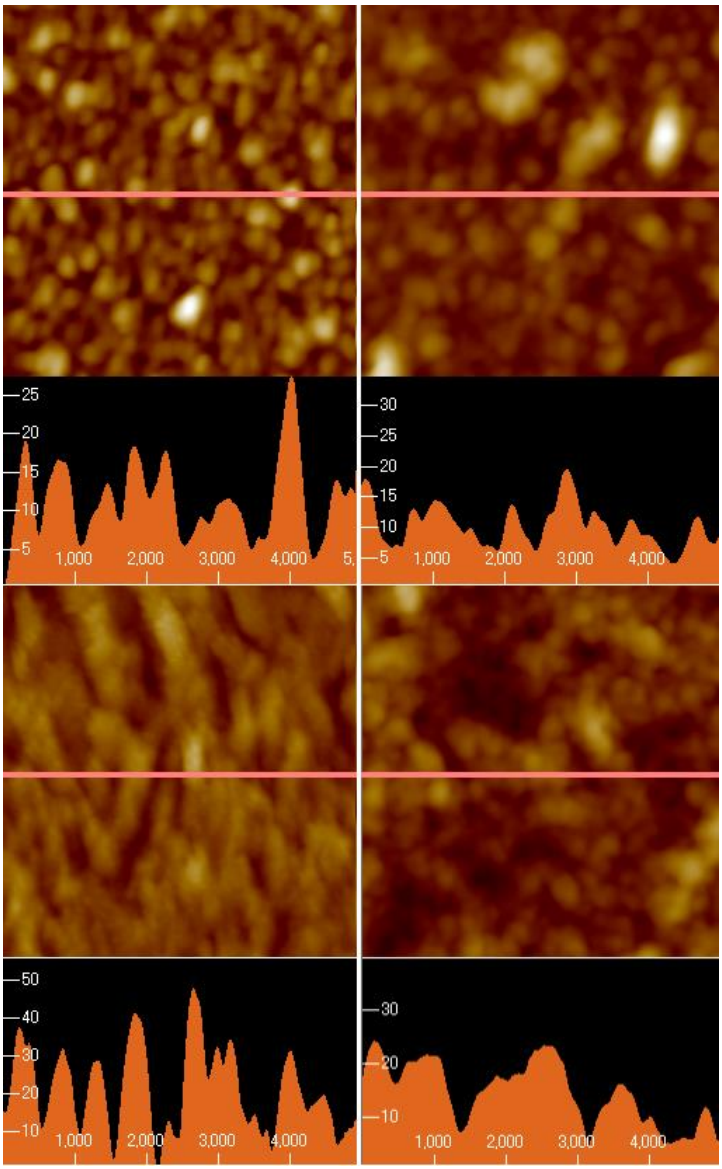

Fig. 1. Surface AFM characterization P3HT films deposited from CB with various solvent additives: CB (top left), DCB (top right), s-TCB (bottom left) and l-TCB (bottom right). AFM images correspond to an area of 5μm x 5μm.

Fig. 1 and Table I summarize the observed changes in morphology of the P3HT films prior to PCBM spin-coating. While the CB films display a typical small crystal morphology, the addition of higher boiling point liquid solvents (DCB and l-TCB) results in a general increase of the P3HT crystal dimensions. In the case of DCB, larger crystals are formed on the surface and addition of l-TCB results in the formation of larger disordered crystal aggregates. On the other hand, in the film prepared from CB with s-TCB as a solvent, the polymer crystals seem to be arranged in a fiber like structure therefore increasing the overall surface roughness of the films.

Table I. P3HT film dimensions measured by AFM for various solvent additives

Solvent additive	bp. (°C)	thickness (nm)	surface roughness, Rz (nm)
Chlorobenzene (CB)	131.0	72.2	14.6
1,2-Dichlorobenzene (DCB)	180.5	70.8	18.3
1,3,5-Trichlorobenzene (s-TCB)	208.0	67.8	32.1
1,2,4-Trichlorobenzene (l-TCB)	214.4	68.4	14.2

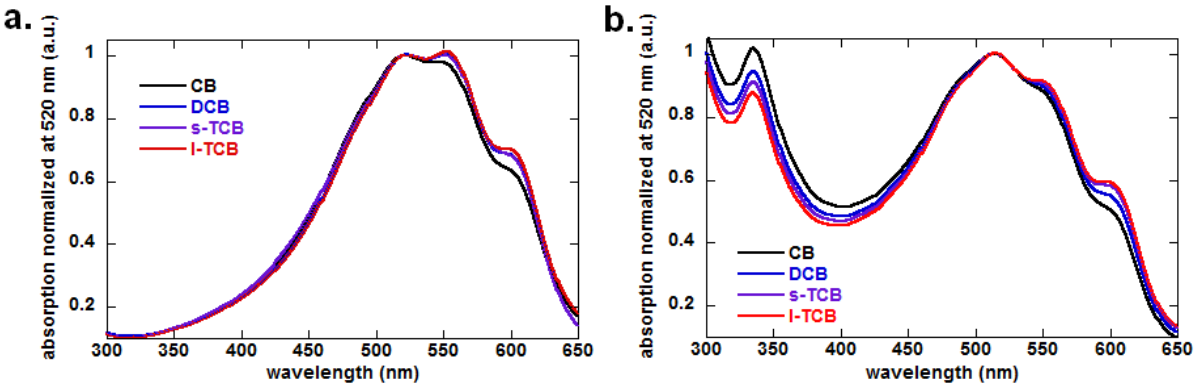

Fig. 2. Absorption spectra of P3HT films deposited from CB with various solvent additives before (a) and after (b) the PCBM deposition and post annealing step at 140°C for 10 min.

The absorption spectra in Fig. 2a further confirm the increase of crystallinity in the films prepared with added higher boiling point solvent. In fact, the typical crystalline shoulders observed around 560 and 610 nm increase relative to the peak at 520 nm with increasing solvent boiling point. While the DCB and s-TCB films have a similar crystallinity (boiling points of 180.5 and 208.0 °C, respectively), the l-TCB (214.4 °C) films display a slightly higher crystallinity. It is worth mentioning that higher crystallinity in P3HT and other similar conjugated polymer films results in increased resistance to infiltration of both PCBM and DCM and therefore should lead to less diffusion of PCBM through the underlying polymer layer.[9)] After PCBM deposition and annealing at 140 °C for 10 min (conditions for device active layer fabrication), some notable changes can be observed in the absorption spectra of the various films (Fig 2b). More specifically, the P3HT absorption peak around 520 nm becomes stronger relative to the shoulder at 560 nm. This is assigned to a combination of two phenomena. First, the absorption tail from PCBM (shoulder around 500 nm) slightly increases the absorption observed around 520 nm in the P3HT:PCBM films. Furthermore, as PCBM molecules diffuse inside the P3HT network, the crystallinity of the P3HT films is disturbed resulting in small changes in relative ratios of the 520 and 560 nm peak intensities. It is worth mentioning that no major changes in absorption spectra were observed before and after annealing of P3HT:PCBM films. The absorption spectra in Fig. 2b clearly exhibit the typical absorption peaks from both P3HT and PCBM. Using the peak intensities at 335 nm (PCBM) and 520 nm (P3HT) and taking into account the absorption coefficients of both materials at these wavelengths, we can approximate the relative P3HT:PCBM ratios in the various thin films. Note that these calculations do not correspond to the P3HT:PCBM weight ratios but are used to qualitatively observe the evolution of the relative concentration of both materials in the active layers. The results, displayed in Table II, clearly indicate that, as expected, PCBM diffusion into P3HT decreases with increasing P3HT crystallinity.

Table II. Relative concentration of P3HT and PCBM in the active layers (P3HT:PCBM)

CB	DCB	s-TCB	l-TCB
1:0.70	1:0.64	1: 0.62	1:0.59

The devices are finalized by evaporating a thin (0.5 nm) layer of LiF followed by a 100 nm thick aluminum layer acting as a reflective electrode and characterized using a sourcemeter (Keithley 2400) and a solar simulator (AM 1.5G, 100 mW/cm^2) at room temperature to extract their photovoltaic performances. Furthermore, the cross-sections of the devices were analyzed by energy dispersive X-ray spectroscopy (EDS) elemental analysis which was carried out with a scanning transmission electron microscope, JEM-ARM200F from JEOL. The acceleration voltage and probe current were 200 kV and 59 pA, respectively to obtain 256 x 256 pixels images with a dwell time of 1 ms/pixel. Each image was accumulated for 120 s to improve the signal to noise ratio. The resulting elemental mappings and sulfur profiles of the active layers are shown in Fig. 3. The sulfur profiles in Fig. 3 relate the changes in sulfur concentration throughout the vertical direction in the active layers. Prior to analyzing the results more carefully, we should note that the devices prepared from CB and DCB additives result in active layer thicknesses around 100 nm while the TCB additives active layer thicknesses are around 80 nm. The difference in thickness may be explained by different wetting ability of the surface with respect to DCM and/or changes in the amounts of PCBM diffusing through the underlying P3HT films.

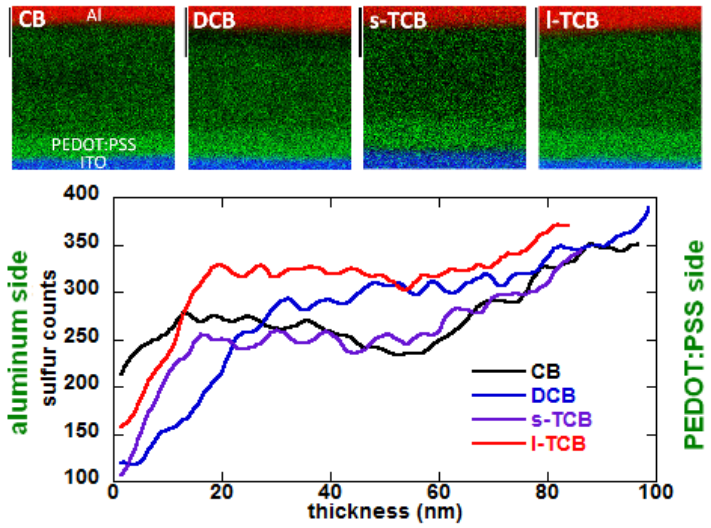

Fig. 3. EDS elemental mapping and active layer sulfur profiles of the P3HT:PCBM DB-PSC prepared using various chlorinated solvent additives. The scale bar (black line) corresponds to 50 nm. The detected elements are indium in blue, sulfur in green and aluminum in red.

Table III and Fig. 4 display the average J-V curves and photovoltaic parameters extracted from 8 devices of each type. The CB devices have a rather flat sulfur profile with a large amount of polymer present at the interface with the top electrode and some PCBM trapped in the center of the active layer. The PCBM most probably diffuses until the bottom of the active layer generating a pseudo-BHJ-PSC which is consistent with previous results on similar device architectures.[7)] The other active layers display an improvement of the vertical concentration gradient. More specifically, in the DCB and s-TCB additive devices, the increased crystallinity of the polymer film leads to a controlled diffusion of the PCBM and a more adequate vertical concentration gradient can be observed (compared to other devices with similar active layer thicknesses). On the other hand, the active layers prepared from l-TCB exhibit a relatively high P3HT concentration at the cathode interface. Together with the decrease of PCBM amount observed previously (Table II), this suggests that only a very thin layer of PCBM is formed on top of the l-TCB P3HT. As the EDS profiles correspond to the

average data over the analyzed surface, we can assume that this thin PCBM layer (around 15 nm) may not be uniform.

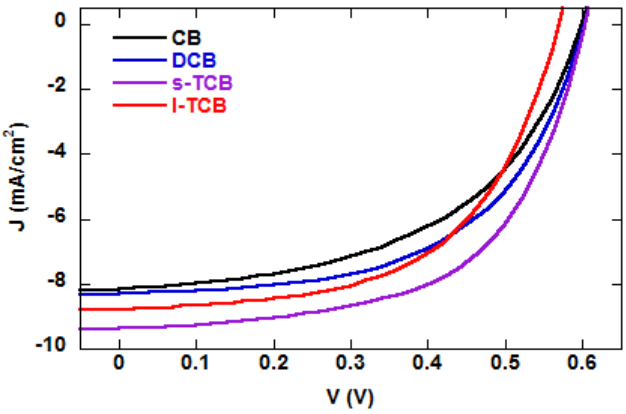

Fig. 4. J-V characteristics of the devices under AM 1.5 (100 mW/cm^2)

Table III. Summary of the device performances under AM 1.5 (100 mW/cm^2)

Solvent additive	bp. (°C)	Jsc (mA/cm^2)	Voc (mV)	FF (%)	PCE (%)	Rs (Ω cm^2)	Rsh (Ω cm^2)
Chlorobenzene (CB)	131.0	8.13	603	51.1	2.50	18.96	723.3
1,2-Dichlorobenzene (DCB)	180.5	8.32	609	55.1	2.79	13.98	1326.7
1,3,5-Trichlorobenzene (s-TCB)	208.0	9.39	607	57.9	3.30	11.71	1185.2
1,2,4-Trichlorobenzene (l-TCB)	214.4	8.79	574	55.8	2.81	13.82	721.4

Furthermore, the addition of l-TCB and the resulting increase in crystallinity, which hinders the penetration of PCBM through the P3HT film, results in a higher degree of separation between both materials (less intermixed layer) and therefore, a lower Jsc compared to the s-TCB devices.

The differences in FF between the various devices can be fully analyzed using the calculated values of their series (Rs) and shunt (Rsh) resistances. In fact, the EDS profiles are well correlated with these calculated values: the two active layers having a higher concentration of P3HT in contact with the cathode, namely, CB and l-TCB devices, have a

Rsh around 720 $\Omega.cm^2$ while the two others, having an adequate concentration gradient profile, display values over 1100 $\Omega.cm^2$. Rs for the CB devices display the highest values as a consequence of their thickness and their inadequate vertical concentration gradient while devices with the same thickness but having a more adequate concentration gradient, namely, DCB devices, exhibit a drop of Rs resulting (together with the increased Rsh) in an increased FF. A similar reasoning can be done when comparing s-TCB and l-TCB devices with the higher Rs calculated for l-TCB devices may be a consequence of the above mentioned non-uniformity of the top PCBM active layer. DCB and l-TCB devices, however, even though their Rsh are fairly different, display similar FF. Both types of device also have similar Rs due to two opposite influences: thicker films with stronger concentration gradients in the case of DCB devices and thinner active layers with less concentration gradient for l-TCB devices. Similarly to our previous experiments and calculations, this suggests that changes in Rs have a greater influence on FF than Rsh variations.[14)] Unexpectedly and although they have a thinner intermixed layer, l-TCB devices display an increased Jsc compared to CB and DCB devices. This is partially related to the fact that the charges percolate to their respective electrodes more efficiently in these thinner active layers but could also be due to a larger amount of donor-acceptor interface in the case of l-TCB. The EDS profile of s-TCB confirms that a large intermixed layer is formed which, also taking into account the low Rs and high Rsh from these devices, explains the higher FF and Jsc obtained.

As demonstrated in previous studies on BHJ-PSC, Voc can be greatly influenced by the P3HT:PCBM ratio and the charge mobilities of both materials.[16,17)] As mentioned in Table II, the amount of PCBM (relative to P3HT) in the devices fabricated in this study decreases with increasing boiling point of the solvent. The trend for Voc observed here can therefore be associated with these changes in P3HT:PCBM ratios. In fact, the Voc values obtained in this study correlate fairly well with a previous study, and, in particular, explain the drop in Voc

observed for active layers containing lower PCBM concentrations (l-TCB). [16] Compared to the reference devices (CB), our best performing devices (s-TCB) display an increase of Jsc and FF of 15.5 and 13.3 %, respectively. Together with a small increase in Voc, this results in a 32% enhancement of the PCE.

In summary, we have demonstrated a simple method based on the use of high boiling point common organic solvents to improve the performances of DB-PSC. In particular, we have verified that an increased crystallinity can be generated by using higher boiling point solvents such as TCB. However, a too high crystallinity leads to a thinner intermixed layer (no diffusion of PCBM inside the P3HT crystalline network) which results in a decrease of Jsc, Voc, FF and PCE. Our best devices were obtained using s-TCB as the chlorinated solvent additives and the PCE was increased to an average of 3.30 % (compare to 2.50 % for CB reference devices). Unlike previously reported studies, this method does not require any post process (e.g. rubbing or structuration of the bottom layer) and is therefore roll-to-roll process compatible.[18] Furthermore, the use of a solid solvent as a crystallizing agent could be applied to higher efficiency polymer materials with low inherent crystallinity and very high PCE can be expected through a control of both the vertical concentration gradient and polymer crystallization.

Acknowledgments

The work was supported by a Grant-in-Aid for Scientific Research on Innovative Areas (No. 20108012, "pi-Space") from the Ministry of Education, Culture, Sports, Science, and Technology, Japan and by JSPS KAKENHI Grant Number 26889029. The authors would like to thank M. Campoy-Quiles (ICMAB-CSIC) for helpful discussions.

References

1) V. Vohra, K. Kawashima, T. Kakara, T. Koganezawa, I. Osaka, K. Takimiya, and H. Murata, Nat. Photonics **9**, 403-408 (2015).

2) Y. Liu, J. Zhao, Z. Li, C. Mu, W. Ma, H. Hu, K. Jiang, H. Lin, H. Ade, and H. Yan, Nat. Commun. **5**, 5293 (2014).

3) J.-D. Chen, C. Cui, Y.-Q. Li, L. Zhou, Q.-D. Ou, C. Li, Y. Li, and J.-X. Tang, Adv. Mater. **27**, 1035-1041 (2015).

4) C. Liu, C. Yi, K. Wang, Y. Yang, R. S. Bhatta, M. Tsige, S. Xiao and X. Gong, Appl. Mater. Interf. **7**, 4928-4935 (2015).

5) B. Yang, T. Yuan and J. Huang, J. Phys. Chem. C **118**, 5196-5202 (2014).

6) M.C. Scharber, and N.S. Sariciftci, Prog. Polym. Sci. **38**, 1929-1940 (2013).

7) K.H. Lee, P.E. Schwenn, A.R.G. Smith, H. Cavaye, P.E. Shaw, M. James, K.B. Krueger, I.R. Gentle, P. Meredith, and P. Burn, Adv. Mater. **23**, 766-770 (2011).

8) A.L. Ayzner, C.J. Tassone, S.H. Tolbert, and B.J. Schwartz, J. Phys. Chem. C **113**, 20050–20060 (2009).

9) J. Seok, T.J. Shin, S. Park, C. Cho, J.-Y. Lee, D.Y. Ryu, M.H. Kim, and K. Kim, Sci. Rep. **5**, 8373 (2015).

10) S. A. Hawks, J. C. Aguirre, L. T. Schelhas, R. J. Thompson, R. C. Huber, A. S. Ferreira, G. Zhang, A. A. Herzing, S. H. Tolbert and B. J. Schwartz, J. Phys. Chem. C **118**, 17412-17425 (2014).

11) A. J. Clulow, C. Tao, K. H. Lee, M. Velusamy, J. A. McEwan, P. R. Shaw, N. L. Yamada, M. James, P. L. Burn, I. R. Gentle and P. Meredith, Langmuir **30**, 11474-11484 (2014).

12) Y. Liu, F. Liu, H.-W. Wang, D. Nordlund, Z. Sun, S. Ferdous and T. P. Russell, Appl. Mater. Interf. **7**, 653-661 (2015).

13) J. C. Aguirre, S. A. Hawks, A. S. Ferreira, P. Yee, S. Subramaniyan, S. A. Jenekhe, S. H. Tolbert and B. J. Schwartz, Adv. Energ. Mater. **5**, 1402020 (2015).

14) V. Vohra, K. Higashimine, S. Tsuzaki, K. Ohdaira, and H. Murata, Thin Solid Films **554**, 41-45 (2014).

15) C. Muller, M. Aghamohammadi, S. Himmelberger, P. Sonar, M. Garriga, A. Salleo, and M. Campoy-Quiles, Adv. Mater. **23**, 2368-2377 (2013).

16) S. S. van Bavel, M. Bärenklau, G. de With, H. Hoppe and J. Loos, Adv. Funct. Mater. **20**, 1458-1463 (2010).

17) O. Ramirez, V. Cabrera and L. M. Reséndiz, Opt. Quant. Electron. **46**, 1291-1296 (2014).

18) V. Vohra, M. Campoy-Quiles, M. Garriga, and H. Murata, J. Mater. Chem. **22**, 20017-20025 (2012).

Fig. 1. Surface AFM characterization P3HT films deposited from CB with various solvent additives: CB (top left), DCB (top right), s-TCB (bottom left) and l-TCB (bottom right). AFM images correspond to an area of 5μm x 5μm.

Fig. 2. Absorption spectra of P3HT films deposited from CB with various solvent additives before (a) and after (b) the PCBM deposition and post annealing step at 140°C for 10 min.

Fig. 3. EDS elemental mapping and active layer sulfur profiles of the P3HT:PCBM DB-PSC prepared using various chlorinated solvent additives. The scale bar (black line) corresponds to 50 nm. The detected elements are indium in blue, sulfur in green and aluminum in red.

Fig. 4. J-V characteristics of the devices under AM 1.5 (100 mW/cm^2)

Table I. P3HT film dimensions measured by AFM for various solvent additives

Table II. Relative concentration of P3HT and PCBM in the active layers (P3HT:PCBM)

Table III. Summary of the device performances under AM 1.5 (100 mW/cm^2)